

## P-y curves from DMT data for piles driven in clay

S. Marchetti, G. Totani, M. Calabrese & P. Monaco  
L'Aquila University, Italy

Proc. 4th Int. Conf. DFI -  
Deep Foundation Inst. on  
Piling and Deep Founda-  
tions, Vol. 1: 263-272.  
Stresa, Italy. Apr. 1991

**ABSTRACT:** The results of two carefully instrumented horizontal loading pile tests in clay are compared with the predictions obtained by existing methods for deriving the P-y curves from DMT data. The piles were "Multiton" mandrel-driven cast-in-situ piles, 57 m long, 0.50 m in diameter. The soil, in its upper part - relevant to the horizontal loading - is soft clay, with a 4 m desiccation crust. The first test pile was loaded with the head free to rotate, the second with the head restrained from rotation. The maximum applied horizontal loads for the two piles were 320 and 420 kN respectively, with corresponding horizontal displacements of approximately 110 mm and 30 mm. The Robertson et al. (1989) method predictions are so close to the observed results that, considering also previous validations, one may be tempted to conclude that this method has solved for good the problem of the linkage between P-y curves and DMT data (for "ordinary" clay, soft to moderately stiff, under static monotonic short-term one-way loading). Of course further validations can only be encouraged. A "simplified formulation", providing similarly accurate predictions, is also presented.

### 1 INTRODUCTION

Most of today's Flat Dilatometer applications concern the evaluation of current geotechnical parameters such as the 1-Dimensional modulus  $M$  and the clay undrained strength  $C_u$ .

However, given the topic of this paper, it may be appropriate to recall that the original stimulus that led to the conception of the Flat Dilatometer was the perceived need of a tool that could help the designer in selecting input parameters in laterally loaded pile calculations. The steps that, starting from the initial idea of a "jacked model-pile deforming inside the soil mass", led to the present design of the Dilatometer, are illustrated in Marchetti, 1977.

The importance for designers of tools that can help in selecting input parameters for laterally loaded piles stems from the small number of practical/reliable alternatives. One of the most used method is the "cubic parabola  $P_u$ - $y_{50}$  method", with  $y_{50}$  derived from  $\epsilon_{50}$  in the laboratory. However, for various reasons (especially vulnerability of  $\epsilon_{50}$  to sample disturbance) and practical constraints (limited number of samples), seldom has the designer available values of  $\epsilon_{50}$  sufficient for quality and quantity.

Features of the DMT that appear favourable for the design of laterally loaded piles are :

- The test provides effectively a large number of measurements, even close to the ground surface, where lateral pile response is mostly influenced.
- The penetration-expansion sequence duplicates, to some extent, the installation-lateral loading process (at least for driven piles).
- The membrane expansion causes the interface soil to move essentially in one direction, and not according to an axially symmetric pattern.

So far, two methods have been developed - to the writers knowledge - for deriving input parameters for laterally loaded piles from DMT data, namely the Robertson et al. method and Gabr & Borden method. Both address the case of monotonic short-term one-way loading. Both methods have been developed/validated based on a limited number of real-scale piles. This paper reports a case history as a contribution in the validation process.

The case history presented here in is part of a major research effort coordinated and sponsored by Icels Pali - Milan, starting in 1990, to monitor the

performance, under various engineering viewpoints, of their "Multiton" piles, recently introduced to the market. In this programme several Multiton piles, 50 to 60 m long, equipped with a variety of internal instruments (inclinator tubings, dilatometer cells on shaft and bottom, extensometer cells) were driven and subjected to a variety of test loadings. Another paper presented to this Symposium (Rocchi et al.) analyzes the pile response to vertical loading.

### 2 SUMMARY OF EXISTING METHODS

This section summarizes the main steps involved in the Robertson et al. method (Robertson et al., 1989) and in the Gabr & Borden method (Gabr & Borden, 1988; Gabr, 1988). For more details the reader is referred to the original papers. Both methods derive the P-y curves from DMT data. They were developed for possible application only to the case of static monotonic short-term one-way loading. Procedures for taking into account cyclic loading are not available yet, and are not considered in this paper.

#### 2.1 DMT P-y curve method by Robertson et al. (1989)

This method is an adaptation of the early methods for estimating P-y curves that utilized soil properties obtained from laboratory testing (Matlock, 1970). The equivalent soil input data required for determining P-y curves are here estimated directly from DMT data.

The equation of the P-y curves is a cubic parabola having the non-dimensional form:

$$\frac{P}{P_u} = 0.5 \cdot (y/y_{50})^{0.33} \quad (2.1)$$

where

- $P_u$  = ultimate soil resistance
- $y_{50}$  = pile deflection corresponding to a mobilization of one-half of the ultimate soil resistance

Restricting herein consideration to the case of cohesive soils, the ultimate soil resistance is evaluated according to Matlock (1970) by means of the

following equation:

$$P_u = N_p \cdot C_u \cdot D \quad (2.2)$$

with

$$N_p = 3 + \frac{\sigma'_{vo}}{C_u} + J \cdot \frac{z}{D} \leq 9 \quad (2.3)$$

where

- $N_p$  = non-dimensional ultimate clay resistance coefficient
- $C_u$  = undrained shear strength (from DMT)
- $\sigma'_{vo}$  = effective vertical stress at depth  $z$
- $J$  = empirical coefficient (0.50 for soft clay; 0.25 for stiff clay. For the case presented it was adopted  $J=0.50$ )
- $D$  = pile diameter

The reference pile deflection,  $y_{50}$ , is evaluated by means of the following equation:

$$y_{50} = \frac{23.67 \cdot C_u \cdot D^{0.5}}{F_c \cdot E_d} \quad (2.4)$$

where

- $F_c$  = empirical factor (suggested value  $F_c=10$ )
- $E_d$  = dilatometer modulus ( $y_{50}$  and  $D$  both in cm)

### 2.2 DMT P-y curve method by Gabr & Borden (1988)

Gabr & Borden (1988) proposed a method for evaluating the coefficient of subgrade reaction,  $K_h$ , from DMT data. Recommendations were also given in order to derive P-y curves from DMT (Gabr, 1988).

The P-y curves are approximated by a hyperbolic tangent function having the non-dimensional form:

$$\frac{P}{P_u} = \tanh \left( \frac{E_{s1} \cdot y}{P_u} \right) \quad (2.5)$$

with

$$E_{s1} = 6.5 \cdot \left( \frac{p_0 - \sigma_{ho}}{b} \right) \cdot D \quad (2.6)$$

where

- $E_{s1}$  = initial tangent soil modulus
- $p_0$  = first DMT reading
- $\sigma_{ho}$  = in situ total horizontal at-rest pressure
- $b$  = half blade thickness = 7 mm

Robertson et al. method, taking into account, in addition, the effects of pile installation by reducing  $C_u$  as a function of OCR. The reduction factor, as suggested by Gabr (1988), may be assumed equal to 2/3 for  $OCR \geq 2$  and ranging from 1 to 2/3 for  $1 \leq OCR < 2$ .

### 3 LOADING TESTS

#### 3.1 Site conditions

The test site is near Livorno, in Northern Italy. The layout of the test piles and of the soundings is shown in Fig.1. Six DMT and one CPT were concentrated within about 6 m from the test piles. A borehole was executed at a distance of about 15 m from the test piles.

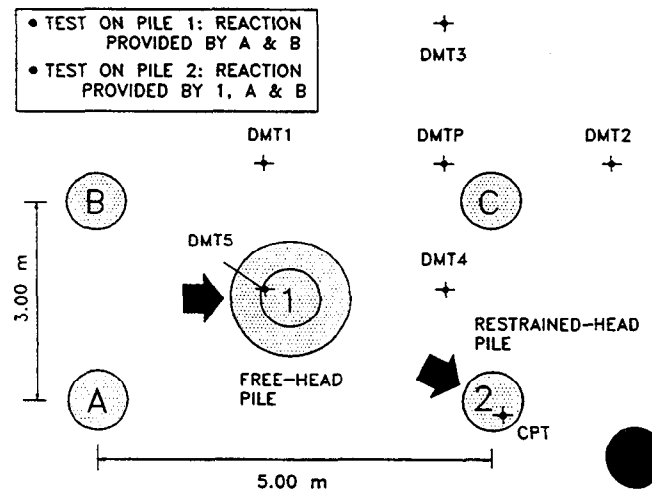


Figure 1. Layout of test piles and soundings.

The geotechnical profile obtained from the results of the borehole is shown in Fig.2. The soil at the site is natural, normally consolidated, saturated soft Holocene clay. The soil in the zone of interest (upper 18 m - relevant to the horizontal loading) is CH clay. Undrained shear strength,  $C_u$ , and constrained modulus,  $M$ , profiles derived from UU triaxial compression tests and oedometer tests in

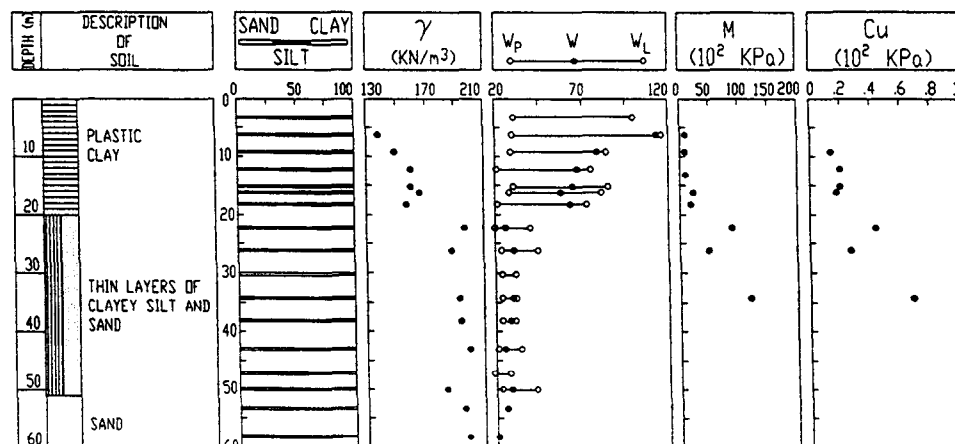


Figure 2. Soil profile and laboratory data at the test site.

# DMT

# CPT

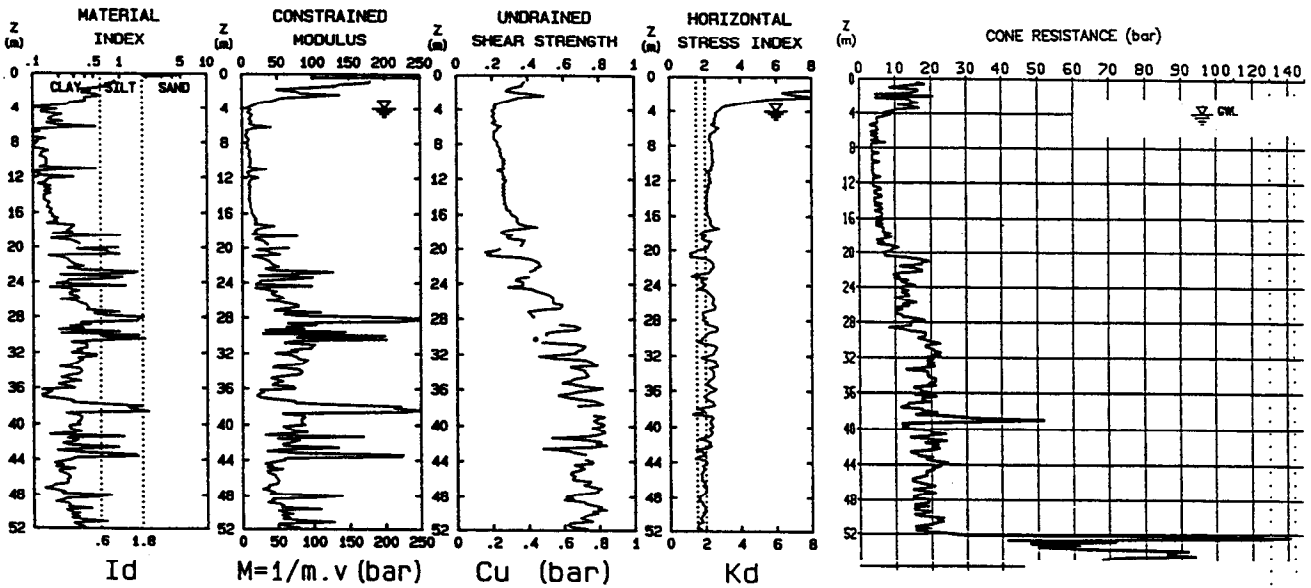


Figure 3. DMT and CPT results.

laboratory, are in good agreement with the DMT results.

Fig.3 shows the results of the cone penetrometer (CPT) sounding obtained with the mechanical cone, and of one of the dilatometer tests (DMT).

Six superimposed profiles of DMT results,  $p_o$ ,  $C_u$  and  $E_d$ , (Fig.4) show that:

- The upper part of the plastic clay has been subjected to desiccation and converted into a "drying crust". This preconsolidation process is the cause of relatively high lateral in situ effective stresses.

The at-rest earth pressure coefficient,  $K_o$ , evaluated from DMT, ranges from 2.4 at a depth of 0.8 m to 1.0 at a depth of 3.0 m.

- The soil in its upper part, immediately below the drying crust, from about 4 to 18 m depth, is remarkably homogeneous and very soft: the undrained shear strength estimated by DMT is as low as 20-30 KPa and the ratio  $C_u/\sigma'_{vo}$  is about 0.27; the sensitivity measured by laboratory vane test is about 10.

The natural groundwater level is 4.0 m below ground surface.

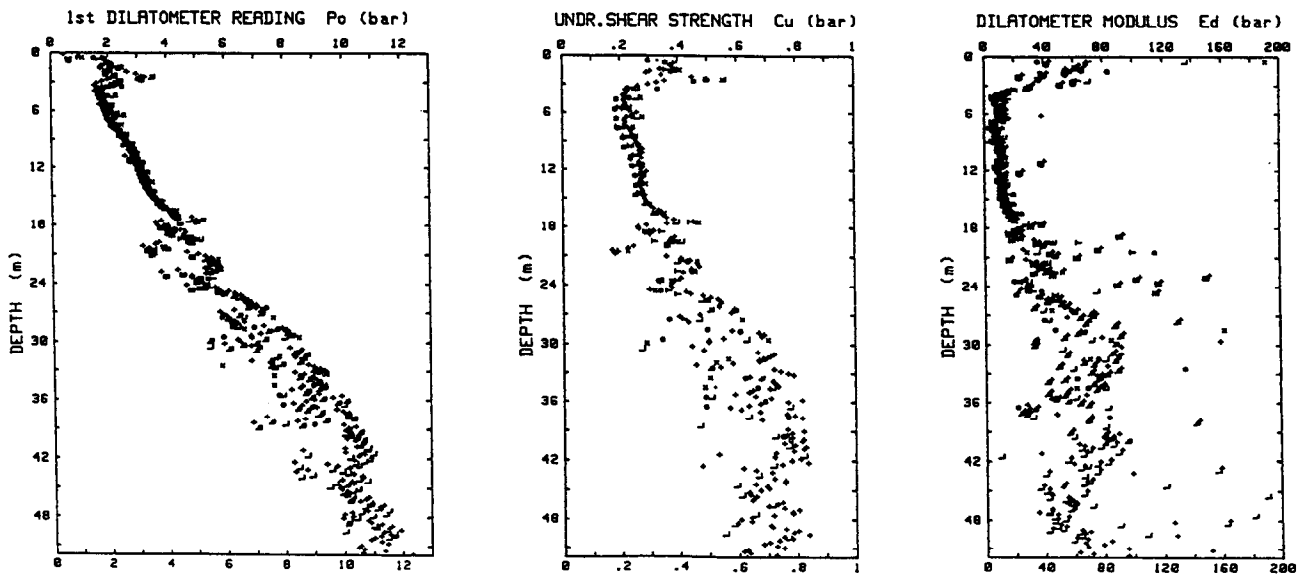


Figure 4. Superimposed profiles of  $p_o$ ,  $C_u$  and  $E_d$  from DMT, DMT1, DMT2, DMT3, DMT4, DMT5.

### 3.2 Test piles

The two test piles were Multiton piles consisting of closed-ended steel pipes, mandrel-driven into the ground, then filled with concrete.

The test piles were driven on May 4 and 15, 1990 respectively. The concrete was cast in place on June 5, 1990.

The characteristics of the test piles are shown in Table 1.

Table 1. Reinforcement and flexural stiffness of the test piles.

z (m)	A <sup>(1)</sup> steel collar (m <sup>2</sup> )	A <sup>(2)</sup> steel tube (m <sup>2</sup> )	A <sup>(3)</sup> reinf. (m <sup>2</sup> )	D <sub>av</sub> reinf. (m)	E <sub>s</sub> tube (KNm <sup>2</sup> )	E <sub>s</sub> reinf. (KNm <sup>2</sup> )	E <sub>c</sub> <sup>(4)</sup> (KNm <sup>2</sup> )	Σ E <sub>s</sub> (KNm <sup>2</sup> )
-0.65	338.6x10 <sup>-4</sup>	99.2x10 <sup>-4</sup>	90.4x10 <sup>-4</sup>	0.4895	782725	50337	838320	167x10 <sup>4</sup>
0.10	-	99.2x10 <sup>-4</sup>	90.4x10 <sup>-4</sup>	0.4895	65625	50337	82796	20x10 <sup>4</sup>
5.35	-	99.2x10 <sup>-4</sup>	36.2x10 <sup>-4</sup>	0.4895	65625	23314	82796	17x10 <sup>4</sup>
11.35	-	99.2x10 <sup>-4</sup>	-	-	65625	-	82796	15x10 <sup>4</sup>
27.00	-	113x10 <sup>-4</sup>	-	-	-	-	-	-
57.00	-	-	-	-	-	-	-	-

NOTE:

- 1) Circular pile cap (not present in the restrained-head pile) was cast inside a steel collar with:  
O.D.=0.910 m I.D.=0.886 m b=0.75 m
- 2) Pile steel tube:  
O.D.=0.508 m I.D.=0.4954 m from 0.10 to 27.00 m depth  
O.D.=0.457 m I.D.=0.4410 m from 27.00 to 57.00 m depth
- 3) Reinforcing steel:  
#20 #24mm from -0.65 to 5.35 m depth  
#8 #24mm from 5.35 to 11.35 m depth
- 4) E<sub>c</sub> (concrete Young's modulus) = 28x10<sup>9</sup> KN/m<sup>2</sup>, from laboratory tests on samples of the cast (in good agreement with estimates inferred from crushing strength of about 30 Mpa)

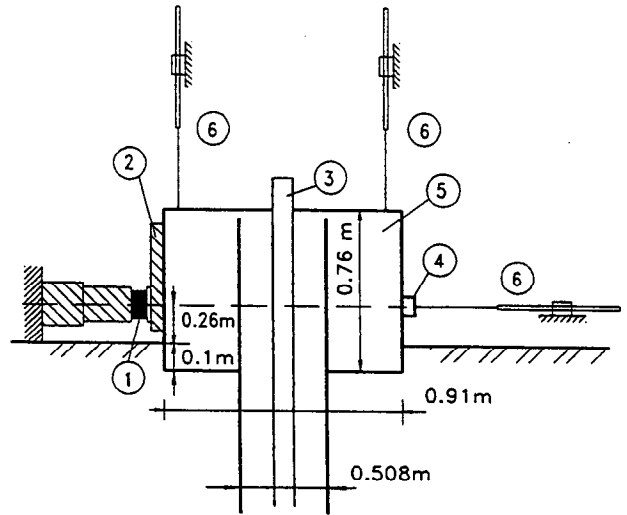
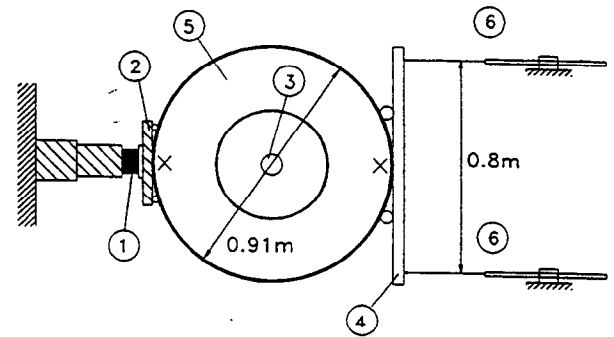


Figure 5. Free-head pile. Plan view and front view.

### 3.3 Instrumentation

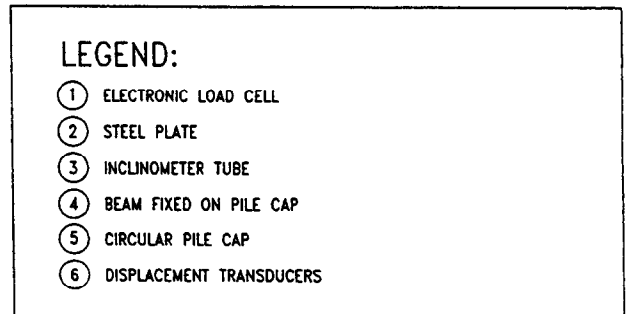
Piles 1 and 2 were instrumented with inclinometer tubings for measuring the horizontal deflections by means of an inclinometer.

The pile horizontal displacements, at the load application level, were also monitored by displacement inductance transducers type "HEM W200" of 0.01 mm accuracy. For the free-head pile additional vertical displacement inductance transducers were placed above the pile head in order to check the pile head rotation. The load applied on both piles was measured by using electronic load cells (maximum load 500 KN) of 0.25 KN accuracy.

All the electronic transducers were connected to a remote computing system. A computer program continuously recorded data on a mini disk.

Only the inclinometer data were recorded manually.

The arrangement of the instrumentation is illustrated in Figs. 5 and 6.



### 3.4 Testing procedures

The lateral loading tests on piles 1 and 2 were performed on July 10, 11 and 12, 1990.

The load on the pile was applied using a hydraulic cylinder reacting against a steel beam welded to piles A and B (see Fig. 1).

- Free-head pile load history (more details in Fig. 7):

0-10-0 KN;  
0-10-20-40-60-80-100-50-0 KN;  
0-50-100-140-180-220-260-130-70-0 KN;  
10 loading-unloading cycles 0-260 KN;  
0-260-300-320-160-0.

- Restrained-head pile load history:

0-50-0 KN;  
0-50-100-140-180-220-260-300-150-0 KN;  
10 loading-unloading cycles 0-320 KN;  
0-300-340-380-420-210-100-0 KN.

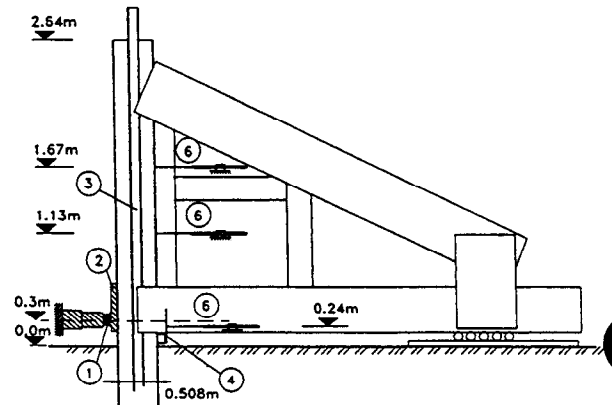


Figure 6. Restrained-head pile. Front view.

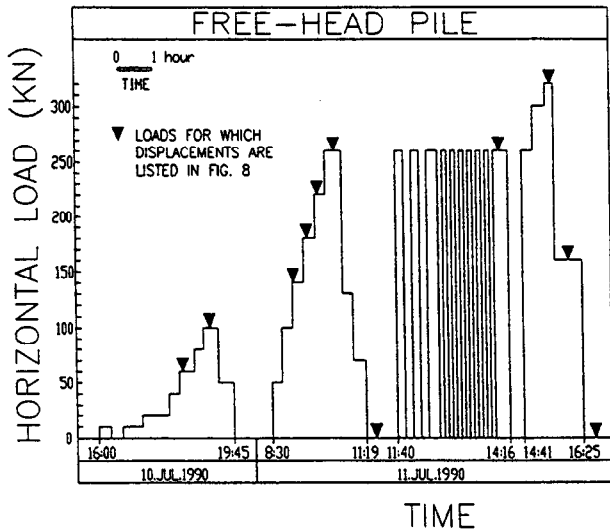


Figure 7. Free-head pile. Load-time history.

#### 4 TEST RESULTS

Inclinometer readings were taken for each load level (increase or decrease) when the pile head displacements, as indicated by the horizontal transducers, reached a nearly constant value. The inclinometer readings were taken at intervals of 0.61 m down to a depth of about 18 m. The inclinometer data were processed with a computer program enabling corrections for temperature effects and other systematic errors, obtaining sets of lateral movements (y) versus depth (z). The results are summarized in Fig. 8.

Lateral load versus pile head displacements measured by the inductance transducers at load application level are shown in Fig. 9 (free-head pile) and in Fig. 10 (restrained-head pile). These automatic measurements are in good agreement with the inclinometer readings, taken independently, confirming the correct behaviour of both instrumentation systems.

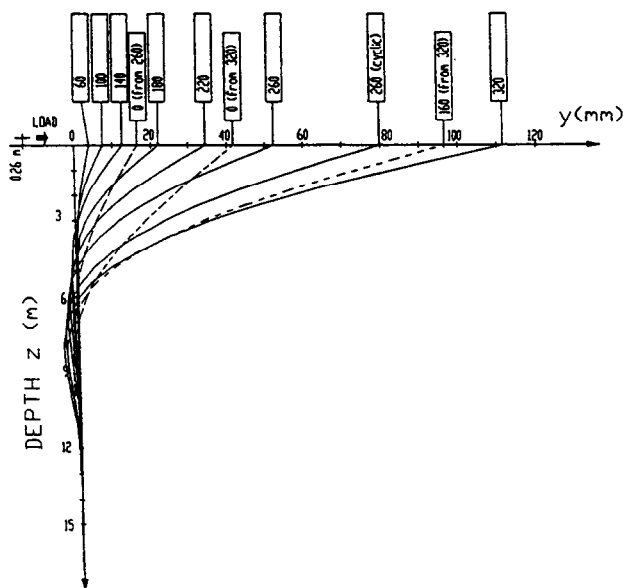


Figure 8. Free-head pile. Lateral deflections from inclinometer data.

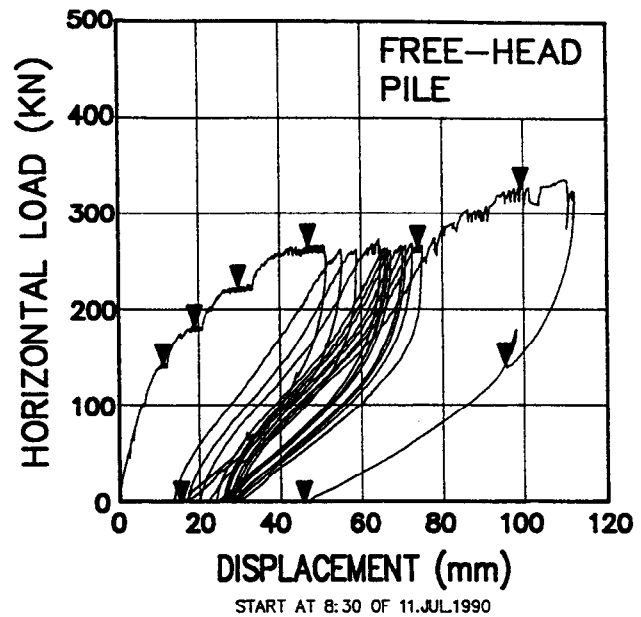


Figure 9. Free-head pile. Displacements measured at 0.26 m above ground level.

#### 5 COMPARISON OF MEASURED VERSUS PREDICTED BEHAVIOUR

##### 5.1 Introduction

The P-y curves predicted by DMT data, according to the two methods discussed in section 2, were used as input for the existing, commercially available, finite difference computer program "LPILE 3.0" (Reese et al., Ensoft Inc., 1989), which calculates pile deflection versus depth at various lateral loads and pile head boundary conditions.

The set of DMT data used for deriving the P-y curves is shown in Table 2. Since DMT provides a near continuous (every 20 cm) record of data and the program can handle only up to 30 P-y curves, DMT data

z (m)	60	100	140	180	220	260	0	260c	320	160	0
	(kN)	(kN)	(kN)	(kN)	(kN)	(kN)	(kN)	(kN)	(kN)	(kN)	(kN)
y	y	y	y	y	y	y	y	y	y	y	y
(mm)	(mm)	(mm)	(mm)	(mm)	(mm)	(mm)	(mm)	(mm)	(mm)	(mm)	(mm)
0.04	4.00	7.60	12.80	22.30	35.00	53.00	16.60	80.70	112.70	97.70	42.10
0.57	3.10	5.60	9.60	17.30	27.80	42.90	14.20	67.50	95.20	83.60	37.20
1.18	2.30	3.80	6.60	12.70	21.10	33.50	11.80	54.70	77.80	69.60	32.30
1.79	1.60	2.30	4.10	8.70	15.20	24.90	9.60	43.00	62.20	56.60	27.50
2.40	1.10	1.30	2.20	5.40	10.10	17.60	7.50	32.50	48.00	44.60	22.90
3.01	0.80	0.60	0.90	2.80	5.90	11.40	5.60	23.50	35.60	33.90	18.40
3.62	0.60	0.40	-0.50	1.10	2.90	6.60	4.00	16.00	25.10	24.70	14.40
4.23	0.50	0.50	-0.80	0.80	0.80	3.00	2.60	9.70	16.50	16.90	10.70
4.84	0.50	0.60	-1.10	-1.10	-0.70	0.30	1.40	4.90	9.50	10.50	7.50
5.45	0.40	0.60	-1.10	-1.40	-1.60	-1.50	0.40	1.40	3.90	5.20	4.40
6.06	0.40	0.50	-0.90	-1.20	-1.90	-2.30	-0.10	-1.40	0.40	1.90	2.50
6.67	0.40	0.40	-0.70	-1.10	-1.90	-2.60	-0.50	-2.60	-1.90	-0.20	0.90
7.28	0.40	0.30	-0.60	-1.00	-1.60	-2.50	-0.70	-3.20	-3.00	-1.90	-0.10
7.89	0.30	0.30	-0.50	-0.80	-1.30	-2.10	-0.70	-3.20	-3.80	-2.90	-1.20
8.50	0.30	0.30	-0.40	-0.60	-1.10	-1.80	-0.70	-2.90	-3.70	-2.90	-1.50
9.11	0.20	0.30	-0.20	-0.30	-0.70	-1.20	-0.50	-2.40	-3.10	-2.50	-1.40
9.72	0.20	0.30	-0.10	-0.10	-0.40	-0.80	-0.30	-1.80	-2.50	-2.00	-1.30
10.33	0.20	0.30	0.30	0.30	-0.10	-0.40	-0.10	-1.30	-1.90	-1.50	-1.10
10.94	0.30	0.30	0.30	0.20	-0.10	-0.20	0.30	-0.60	-1.00	-0.80	-0.50
11.55	0.30	0.30	0.20	0.20	0.10	0.10	0.30	-0.40	-0.60	-0.50	-0.40
12.16	0.20	0.30	0.10	0.20	0.10	0.20	0.30	-0.20	-0.30	-0.30	-0.20
12.77	0.20	0.30	0.20	0.20	0.20	0.20	0.20	-0.20	-0.30	-0.30	-0.30
13.38	0.20	0.20	0.10	0.20	0.10	0.20	0.30	0.00	-0.10	0.00	0.00
13.99	0.20	0.20	0.20	0.20	0.20	0.20	0.20	0.00	-0.10	-0.10	-0.10
14.59	0.10	0.20	0.10	0.10	0.10	0.00	-0.10	-0.20	-0.20	-0.30	-0.30
15.20	0.10	0.10	0.00	-0.30	-0.20	-0.20	-0.20	-0.20	-0.30	-0.30	-0.30
15.81	0.00	-0.10	-0.10	-0.10	-0.10	-0.10	-0.10	-0.10	-0.20	-0.20	-0.20
16.42	0.10	0.10	-0.10	-0.20	-0.10	-0.20	-0.20	-0.20	-0.30	-0.30	-0.30
17.03	0.00	0.00	0.00	0.00	0.00	-0.10	0.10	0.10	0.00	0.00	0.10
17.64	0.00	0.00	0.00	0.00	0.00	0.00	0.00	0.00	0.00	0.00	0.00

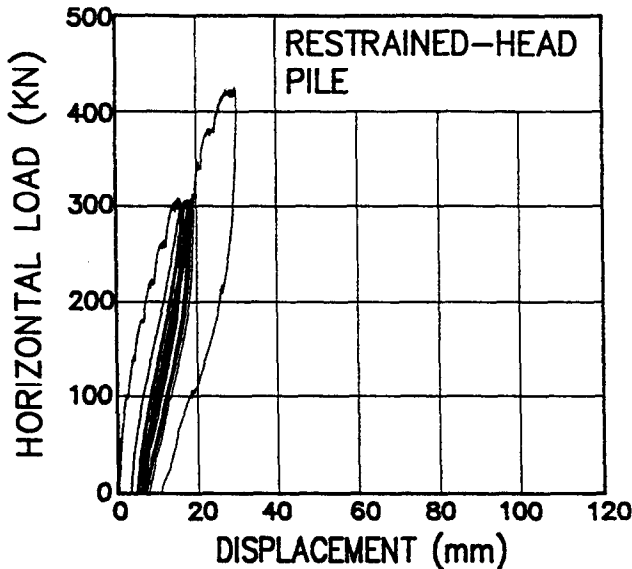


Figure 10. Restrained-head pile. Displacements measured at 0.24 m above ground level.

were averaged into a maximum of 30 corresponding layers.

Some representative P-y curves obtained at various depths by the two methods are shown in Fig. 11.

The analysis was carried out for the following values of the lateral load: 0-60-100-140-180-220-260 KN for the free-head pile; 0-50-100-140-180-220-260-300 KN for the restrained-head pile.

The predicted behaviour was then compared to the experimental data obtained from lateral loading tests.

### 5.2 Free-head pile

A comparison between calculated and measured pile deflections at ground level, as a function of the applied load, is shown in Fig. 12.

Calculated and measured pile deflections versus depth are shown in Fig. 13 under lateral loads of 100, 180, 220 and 260 KN respectively.

It can be seen that the deflections calculated by the Robertson et al. method are in quite good agreement with the measured values under all load levels at all depths. The average difference between predicted and observed displacements at 30 different depths, for 6 values of the horizontal load, was  $\pm 0.5$  mm.

Table 2. Numerical values of DMT data used in the calculation.

Z (m)	$P_o$ (bar)	$\sigma'_{vo}$ (bar)	U (bar)	$E_D$ (bar)	$K_o$ (-)	OCR (-)	$C_u$ (bar)
0.2	1.48	0.03	0.00	235	0.0	0.00	0.00
0.4	0.64	0.07	0.00	42	0.0	0.00	0.00
0.8	2.06	0.14	0.00	62	2.4	23.52	0.38
1.0	2.11	0.17	0.00	66	2.1	17.29	0.37
1.2	2.23	0.20	0.00	53	1.9	14.22	0.37
1.4	2.07	0.24	0.00	55	1.7	10.04	0.33
1.6	1.94	0.27	0.00	40	1.5	7.39	0.29
1.8	1.92	0.30	0.00	24	1.4	6.09	0.28
2.0	2.25	0.33	0.00	37	1.4	6.69	0.34
2.2	2.85	0.37	0.00	37	1.6	8.34	0.44
2.4	3.17	0.40	0.00	60	1.6	8.58	0.49
2.6	2.43	0.43	0.00	51	1.3	5.01	0.35
2.8	2.31	0.47	0.00	31	1.2	4.11	0.32
3.0	2.16	0.50	0.00	30	1.0	3.35	0.29
3.2	1.96	0.53	0.00	28	0.93	2.62	0.25
3.4	1.78	0.56	0.00	17	0.82	2.05	0.22
3.6	1.73	0.59	0.00	15	0.77	1.81	0.21
3.8	1.79	0.62	0.00	9	0.76	1.76	0.22
4.0	1.79	0.65	0.00	6	0.73	1.64	0.21
4.2	1.73	0.66	0.02	11	0.69	1.50	0.20
4.4	1.79	0.67	0.04	8	0.70	1.52	0.21
4.6	1.84	0.68	0.06	8	0.70	1.52	0.21
4.8	1.83	0.69	0.08	13	0.68	1.45	0.20
5.0	1.88	0.70	0.10	11	0.68	1.46	0.21
5.2	1.89	0.71	0.12	9	0.67	1.41	0.21
5.4	1.99	0.72	0.14	9	0.69	1.47	0.22
5.6	1.88	0.73	0.16	13	0.64	1.29	0.20
5.8	2.09	0.74	0.18	9	0.69	1.48	0.22
6.0	2.28	0.75	0.20	13	0.73	1.66	0.25
6.2	2.20	0.76	0.22	37	0.69	1.50	0.23
6.4	2.23	0.78	0.24	13	0.69	1.48	0.23
6.6	2.09	0.79	0.26	6	0.63	1.27	0.21
6.8	2.09	0.80	0.28	8	0.62	1.23	0.21
7.0	2.14	0.81	0.30	6	0.62	1.24	0.21
7.2	2.14	0.81	0.32	6	0.61	1.20	0.21
7.4	2.19	0.82	0.34	6	0.61	1.21	0.21
7.6	2.29	0.83	0.36	9	0.63	1.27	0.22
7.8	2.39	0.84	0.38	8	0.65	1.33	0.23
8.0	2.39	0.85	0.40	8	0.64	1.29	0.23
8.2	2.44	0.86	0.42	8	0.64	1.30	0.23
8.4	2.49	0.87	0.44	8	0.64	1.30	0.24
8.6	2.59	0.88	0.46	6	0.66	1.36	0.25
8.8	2.59	0.89	0.48	9	0.64	1.32	0.24
9.0	2.63	0.90	0.50	11	0.65	1.32	0.25

Z (m)	$P_o$ (bar)	$\sigma'_{vo}$ (bar)	U (bar)	$E_D$ (bar)	$K_o$ (-)	OCR (-)	$C_u$ (bar)
9.2	2.69	0.91	0.52	9	0.65	1.33	0.25
9.4	2.74	0.92	0.54	9	0.65	1.34	0.25
9.6	2.79	0.93	0.56	9	0.65	1.35	0.26
9.8	2.88	0.93	0.58	11	0.67	1.40	0.27
10.0	2.83	0.94	0.60	11	0.64	1.31	0.26
10.2	2.93	0.95	0.62	11	0.66	1.36	0.27
10.4	2.88	0.96	0.64	11	0.63	1.28	0.26
10.6	2.93	0.97	0.66	11	0.63	1.28	0.26
10.8	2.99	0.98	0.68	9	0.64	1.29	0.27
11.0	2.75	0.99	0.70	39	0.56	1.06	0.23
11.2	2.98	1.01	0.72	13	0.61	1.21	0.26
11.4	2.99	1.02	0.74	8	0.60	1.18	0.26
11.6	3.04	1.03	0.76	9	0.61	1.19	0.26
11.8	3.14	1.04	0.78	9	0.62	1.23	0.27
12.0	3.12	1.05	0.80	24	0.60	1.18	0.26
12.2	3.28	1.06	0.82	13	0.63	1.28	0.28
12.4	3.18	1.07	0.84	11	0.60	1.16	0.27
12.6	3.18	1.08	0.86	11	0.59	1.13	0.26
12.8	3.29	1.09	0.88	9	0.60	1.18	0.27
13.0	3.23	1.10	0.90	13	0.58	1.11	0.26
13.2	3.28	1.11	0.92	11	0.58	1.11	0.27
13.4	3.28	1.12	0.94	13	0.57	1.08	0.26
13.6	3.33	1.13	0.96	11	0.57	1.09	0.27
13.8	3.33	1.14	0.98	13	0.56	1.06	0.26
14.0	3.38	1.15	1.00	11	0.57	1.06	0.27
14.2	3.43	1.16	1.02	11	0.57	1.07	0.27
14.4	3.43	1.17	1.04	11	0.56	1.04	0.27
14.6	3.48	1.18	1.06	11	0.56	1.05	0.27
14.8	3.53	1.19	1.08	13	0.56	1.06	0.27
15.0	3.58	1.21	1.10	13	0.57	1.06	0.28
15.2	3.63	1.22	1.12	13	0.57	1.06	0.28
15.4	3.68	1.23	1.14	13	0.57	1.07	0.28
15.6	3.78	1.24	1.16	15	0.58	1.10	0.30
15.8	3.83	1.25	1.18	15	0.58	1.11	0.30
16.0	3.93	1.26	1.20	15	0.59	1.14	0.31
16.2	4.08	1.28	1.22	17	0.61	1.21	0.33
16.4	4.18	1.29	1.24	17	0.62	1.24	0.34
16.6	4.22	1.30	1.26	20	0.62	1.24	0.34
16.8	4.27	1.31	1.28	19	0.62	1.25	0.34
17.0	4.37	1.32	1.30	20	0.63	1.28	0.35
17.2	4.58	1.34	1.32	17	0.66	1.38	0.38
17.4	5.05	1.35	1.34	39	0.73	1.66	0.45
17.6	4.46	1.36	1.36	31	0.62	1.24	0.36
17.8	3.97	1.37	1.38	24	0.52	0.92	0.28

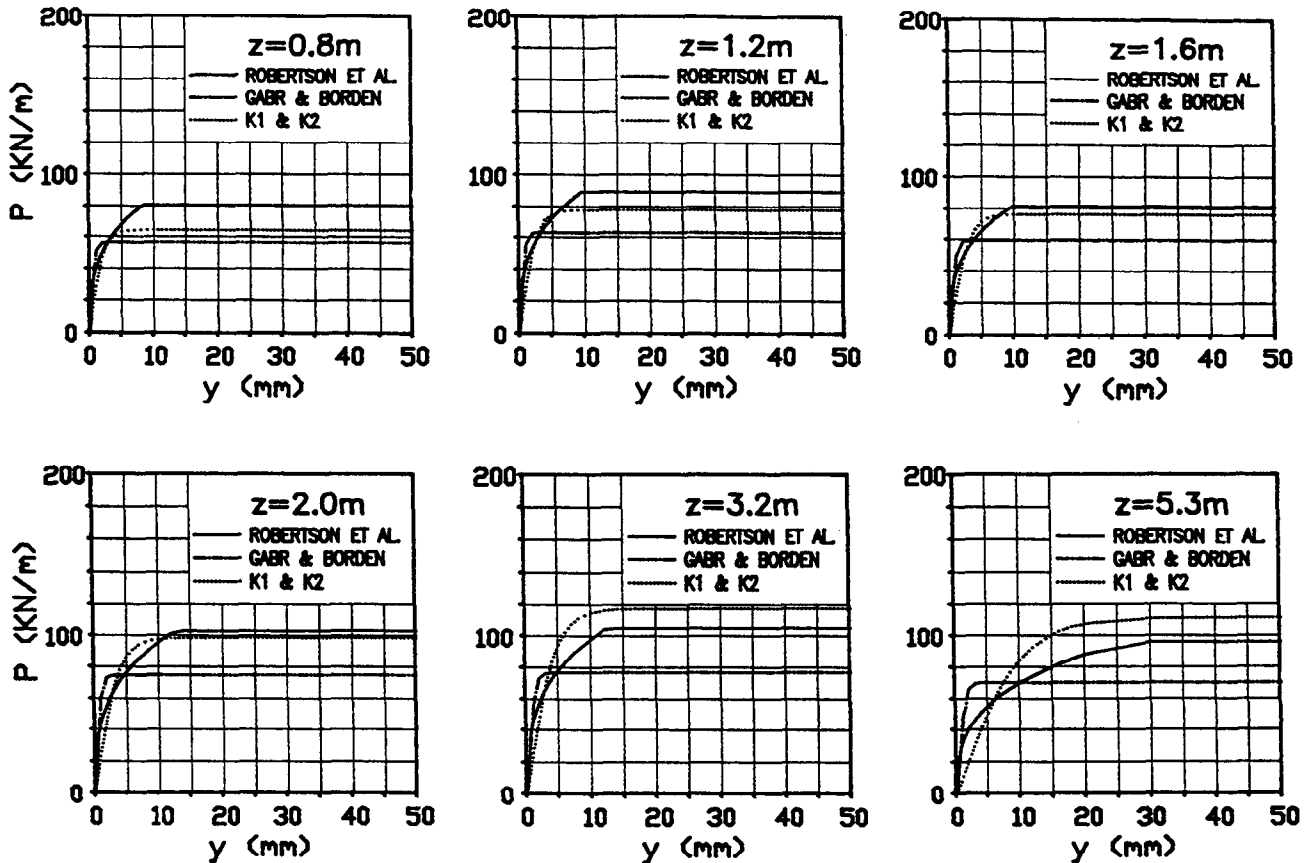


Figure 11. Representative P-y curves from DMT data according to various procedures.

The Gabr & Borden method (assuming a reduction factor of  $C_u$  equal to  $2/3$  for  $OCR \geq 2$ ), overestimates the deflections under large loads and underestimates them at lower loads, as shown in Figs. 12 and 13. This is probably due to the fact that the computed values of  $P_u$ , controlling the behaviour at large loads, are too low and the initial tangent soil modulus, which determines the initial shape of the P-y curve, is too high for the examined case. A second run was made calculating  $P_u$  without any reduction of  $C_u$ : the deflections predicted in this way resulted closer to the measured values, but the error was still significant, especially at lower loads. It is possible to conclude that, for the examined site conditions, the reduction of  $C_u$  as a function of OCR, introduced by Gabr (1988) for a particular test site, is too severe, while the initial soil modulus is too high. One may wonder if part of this disagreement may be explained with the fact that this method does not make full use of the DMT information. In fact the method uses  $p_0$  both to infer  $C_u$  and to select initial stiffness, leaving unused  $E_b$ , that, presumably, has a stronger link with stiffness than  $p_0$ .

### 5.3 Restrained-head pile

A comparison between calculated and measured pile deflections at ground level, as a function of the applied load, is shown in Fig. 14.

Calculated and measured pile deflections versus depth are shown in Fig. 15 under a lateral load of 300 KN.

The deflections predicted by both methods are in excess at large loads (260-300 KN), while, at lower loads, they are in better agreement with the measured values.

Some uncertainties in the evaluation of the predicted versus measured behaviour derive from the

fact that the pile head was not perfectly restrained from rotation during the loading test, due to a settlement of the reaction pad, as signaled by the inclinometer readings. The influence of such "anomalous" boundary condition at the pile head cannot readily be evaluated.

### 6 ALTERNATIVE PROCEDURES. K1 & K2 FORMULATION

The Robertson et al. procedure, being a first attempt, was wisely conceived as an adaptation of an earlier, time-tested method, namely the "cubic parabola  $P_u$ - $y_{50}$  method". One may wonder if, dropping some "inherited steps", may lead to a more straightforward procedure and/or to closer predictions and/or to a smaller number of subjective choices. In particular, some "unnatural" or lengthy steps in the "adapted cubic parabola method" are the following:

a)  $E_b$  is first converted into  $E_i$  via the empirical factor  $F_c=10$ . Then  $E_i$  is used to evaluate  $e_{50}$  (of a UU triaxial specimen), under the added assumption of an hyperbolic stress-strain curve tending to  $C_u$  - estimated from DMT  $p_0$ . Finally  $e_{50}$  is converted to  $y_{50}$  with Eq. 3 of the mentioned reference (Robertson et al., 1989), containing the empirical coefficient  $B=14.2$ .

b) Of the two parameters controlling the cubic parabola,  $P_u$  has the clear physical meaning of ultimate value of P, and its expression does not contain deformation parameters.  $y_{50}$ , instead, is a "coupled" parameter, because, for a given  $y_{50}$ , the slope of the resulting P-y curve increases with  $P_u$ . However, if  $E_b$  is seen essentially as linked to stiffness, it may be preferable a formulation in which the first portion of the P-y curve is controlled solely by  $E_b$ .

c) Relating  $y_{50}$  to  $e_{50}$  involves, besides the

# FREE-HEAD PILE

Figure 12. Free-head pile. Predicted versus measured lateral displacements at ground surface.

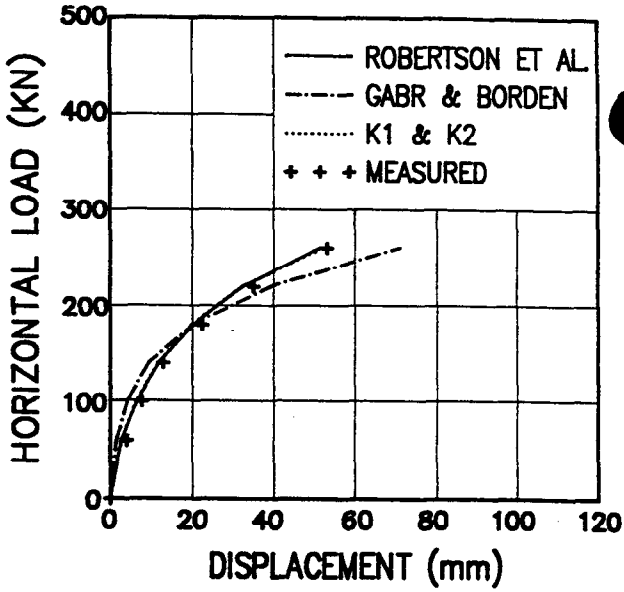
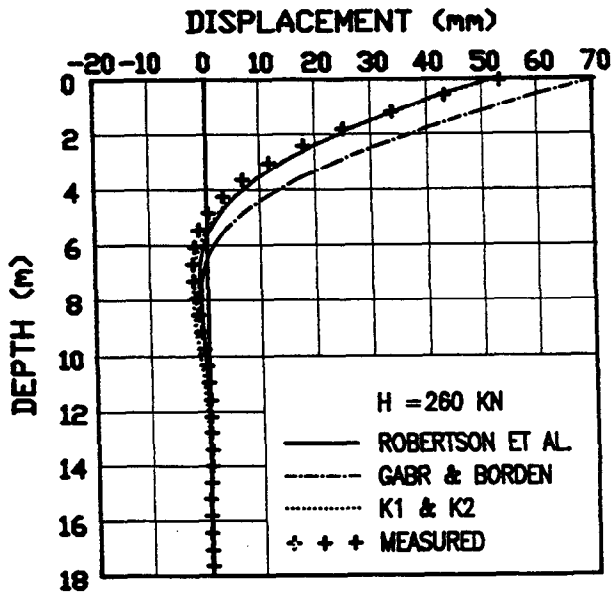
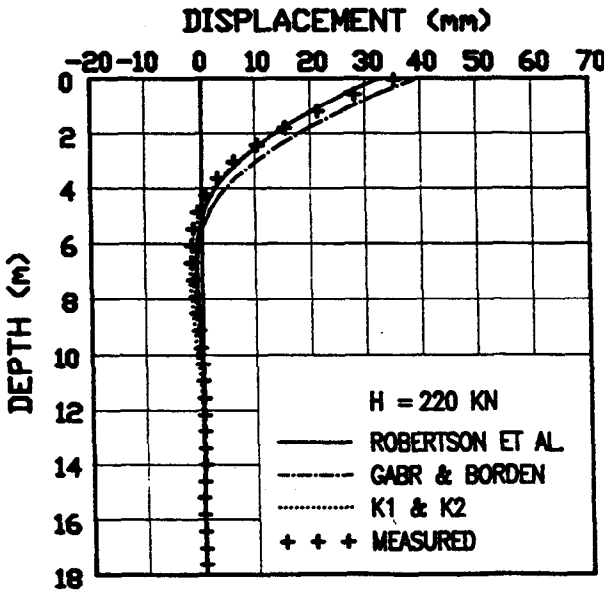
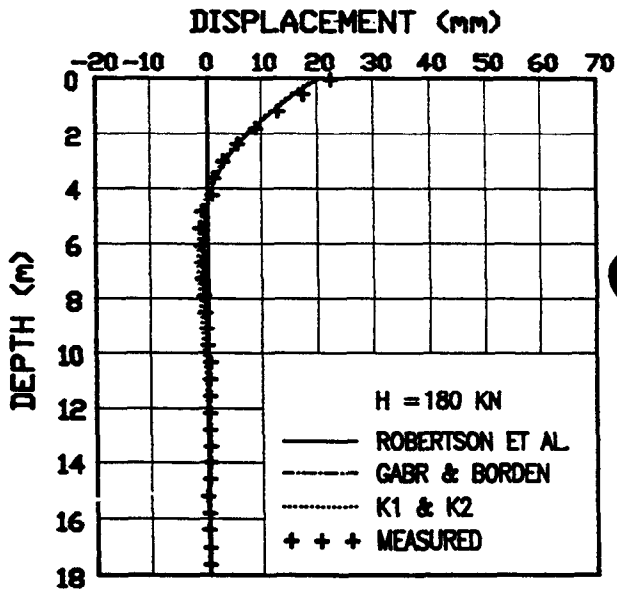
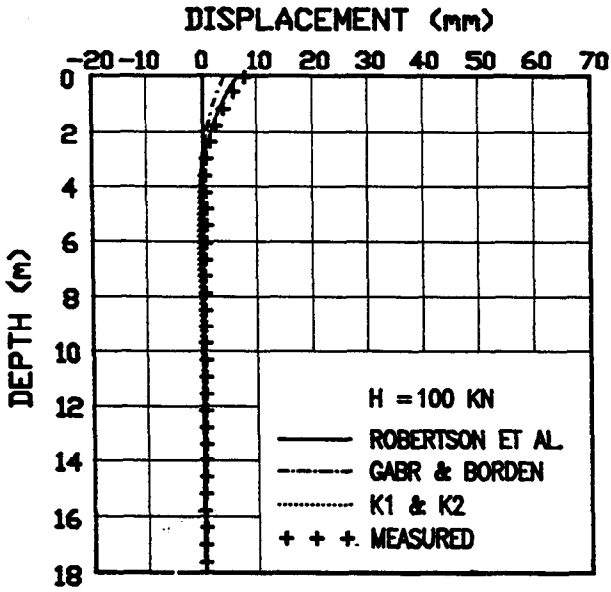


Figure 13. Free-head pile. Predicted versus measured pile axis deflections at various loads.





# RESTRAINED-HEAD PILE

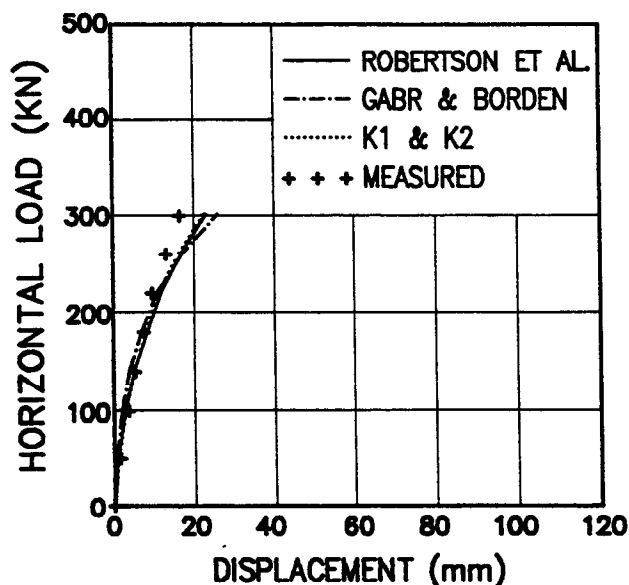


Figure 14. Restrained-head pile. Predicted versus measured lateral displacements at ground surface.

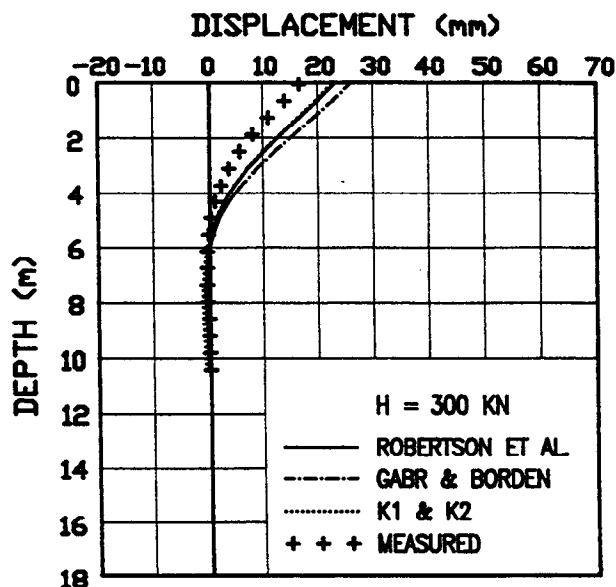


Figure 15. Restrained-head pile. Predicted versus measured pile axis deflections at various loads.

empirical factor  $B$ , the tacit additional assumption of at least some resemblance between the stress-strain curve of a triaxial UU specimen and the "integral" P-y curve opposed by all soil elements reacting against the pile.

In search of a more straightforward procedure, various formulations of the P-y curves were scrutinized, assuming a correlation between  $E_b$  and either  $E_s$  initial or  $E_s$  secant ( $E_s$  secant = ratio P/y at a fixed relative pile displacement  $y/D$ ). Runs were carried out for  $y/D = 0.5\%$ ,  $1\%$ ,  $1.5\%$ .

The best fit of the observed displacements (made for the free-head pile) was obtained by adopting the following hyperbolic tangent law:

$$\frac{P}{P_u} = \tanh \left( \frac{E_{s1} \cdot y}{P_u} \right) \quad (6.1)$$

with

$$P_u = \alpha \cdot K_1 \cdot (p_0 - u_0) \cdot D \quad (6.2)$$

$$E_{s1} = \alpha \cdot K_2 \cdot E_b \quad (6.3)$$

$$K_1 = 1.24 \quad K_2 = 10$$

$$\alpha = \frac{1}{3} + \frac{2}{3} \cdot \frac{z}{7 \cdot D} \leq 1 \quad (6.4)$$

The reduction factor  $\alpha$  given by Eq. 6.4 is a simplified translation of Matlock's Eq. 2.3. It becomes 1 for  $z=7D$ .

Eq. 6.2 above expresses  $P_u$  in terms of its "parent" parameter  $p_0$  ( $C_u$  interpreted by DMT derives directly from  $p_0$ ).

Eq. 6.1 through 6.4 define completely a P-y curve at each depth where  $p_0$  and  $E_b$  are available.

The best-fit search of  $K_1$  &  $K_2$  was carried out as follows. Trial values were assigned both to  $K_1$  &  $K_2$ .

Each pair  $K_1$  &  $K_2$ , fed into Eq. 6.2 and 6.3, defines a complete set of P-y curves. These curves were used to compute theoretical  $y(z)$  for horizontal loads equal to: 60, 100, 140, 180, 220, 260 kN for the free-head pile. The differences (absolute values) between these theoretical displacements and the observed ones (at all depths listed in Fig. 8, for a total of 180 terms  $\delta y$ ) were summed up, thus obtaining  $\sum |\delta y|$ . This sum was used as an index of the predictive capability of that  $K_1$  &  $K_2$  pair. In this way the values of  $K_1$  and  $K_2$  for which the sum is low yield "well balanced"  $y(z)$  predictions, for both low and high horizontal loads. For the pair  $K_1=1.24$ ,  $K_2=10$ ,  $\sum |\delta y| \approx 100$  mm. This value is nearly equal to the one obtained by Robertson et al. procedure and better than the one obtained by Gabr & Borden method.

The good accuracy of the "predictions" made with the "K1 & K2" method is illustrated by the curves shown in Figs. 12 and 13.

NOTE: Eq. 2.4, obtained by Robertson et al., incorporating findings by several researchers, when combined with Eq. 2.2, results in steeper P-y curves as  $D$  increases, for a given soil. If one wants to key-in the same diameter effect into the  $K_1$  &  $K_2$  formulation, one has just to multiply the value  $K_2=10$  (found for  $D=0.5$  m) by the factor  $(D/0.5 \text{ m})^{0.5}$ . For example for  $D=0.5, 1, 2$  m,  $K_2$  would become 10, 14.1, 20 respectively. No correspondent adjustment is needed for  $P_u$  since the  $P_u$  dependence from  $D$  is already accounted for by Eq. 6.2.

## 7 CONCLUSIONS

The case history presented in this paper - horizontal pile loading tests on two well instrumented piles in clay - has enabled a detailed comparison between behaviour observed and predicted by various methods.

Particularly favourable, from the experimental viewpoint, was the circumstance that the type of pile tested has a considerable structural capacity to horizontal loading, in relation to its diameter  $D=0.5$  m. The possibility of applying high horizontal loads

has enabled mobilization of the P-y curves up to failure, and well beyond, for a depth of several meters.

From the comparison predicted-versus-measured behaviour the writers draw the following conclusions:

a) The Robertson et al. (1989) method, applied strictly in the form suggested by the Authors, predicted the observed results with amazing accuracy (average difference between predicted and observed displacements at 30 depths, for 6 values of horizontal load  $\approx 0.5$  mm). If it also considered:

- The independence between the loading tests utilized to develop the method and those described in this paper
- Previous favourable independent validations carried out by the developers of the method

one may be tempted to conclude that this method has solved for good the problem of the linkage between P-y curves and DMT data (for "ordinary" clay, soft to moderately stiff, under static monotonic short-term one-way loading). Of course further validations can only be encouraged.

b) The Gabr & Borden (1988) method, has led, in this case, to less accurate predictions, possibly because developed for relatively stiff OC clay, which is not the present case. One may wonder if such outcome has anything to do with the fact that it does not make full use of the DMT information. In fact the method uses  $p_0$  both to infer  $C_u$  and to select initial stiffness, leaving unused  $E_D$ , that, presumably, has a stronger link with stiffness than  $p_0$ .

c) The Robertson et al. procedure, being a first attempt, was obtained as an adaptation of earlier methods. Some work has then been carried out to see if, dropping some "inherited steps", would lead to a more straightforward procedure and/or to closer predictions and/or to a smaller number of subjective choices. After examining various procedures for deriving the P-y curves from DMT data, a quite satisfactory "simplified" procedure was found, based on a two-parameter ( $E_{s1}$  and  $P_u$ ) hyperbolic tangent law, with  $E_{s1}$  and  $P_u$  linked separately to  $E_D$  and  $p_0$  by a pair of constants ( $K_1$  &  $K_2$ ).

This approach, after a best fit study aimed at identifying the best pair  $K_1$  &  $K_2$ , yielded predictions of accuracy similar to the Robertson et al. method. The fact that relaxing the constraints of earlier methods did not result in improved predictions, indicates (somewhat reassuringly) that there is not much room (nor need, in this case) for improvement. On the other hand a potential advantage of the  $K_1$  &  $K_2$  approach is simplicity and a reduced number of subjective choices.

d) Independently from the method used, it is considered of significance the fact that, at least for the pile-soil analyzed, it emerged very consistently:  $P_u = 1.24 (p_0 - u_0) D$ , where  $P_u$  is the value before the reduction factor  $\alpha$ . If this relation (which, on the other hand, is well in line with previous correlations linking  $C_u$  to  $p_0$  and  $P_u$  to  $C_u$ ) is confirmed by future experience, there is the potential of skipping one step in the correlation chain.

#### ACKNOWLEDGMENTS

Icels Pali active collaboration and support are gratefully acknowledged. The writers also express their appreciation to R. Scalorbi for his skill and care in reducing the inclinometer data and to L. Fatigati for his technical assistance during tests execution.

#### REFERENCES

- Ensoft Inc. 1989. Computer program LPILE, Version 3.0. Austin (Texas).
- Gabr, M.A. 1988. Application of dilatometer for pile design. Evaluation of subgrade reaction for lateral pile analysis in clay. Norwegian Geotechnical Institute, Oslo, Norway. Report S21610-4.
- Gabr, M.A. & Borden, R.H. 1988. Analysis of load deflection response of laterally loaded piers using dilatometer test (DMT). International Symposium on Penetration Testing ISOPT-1. Orlando. Proc. Vol.1:513-520.
- Lunne, T. et al. 1989. SPT, CPT, Pressuremeter Testing and Recent Developments on In Situ Testing. Proc. 12th ICSMFE, General Rep. Sess. 2, Rio de Janeiro.
- Marchetti, S. 1977. Devices for In Situ Determination of Soil Modulus Es. Proc. of 9th ICSMFE, Tokio, Specialty Session 10:197.
- Marchetti, S. 1980. In Situ Tests by Flat Dilatometer. Journal of the Geotechnical Engineering Division, ASCE, Vol. 106, No. GT3, Proc. Paper 15290:299-321.
- Matlock, H. 1970. Correlation for Design of Laterally Loaded Piles in Soft Clay. Proc. of the II Offshore Technical Conference, Houston, TX, Vol. 1:577:594.
- Reese, L.C. & Wang, S. 1989. Documentation of Computer program LPILE 3.0. Austin: Ensoft Inc.
- Robertson, P.K., Davies, M.P. & Campanella, R.G. 1989. Design of Laterally Loaded Driven Piles Using the Flat Dilatometer. Geotechnical Testing Journal. GTJODJ, Vol. 12, No. 1:30-38